

# Characterization of polymeric vesicles of poly(sodium 11-acrylamidoundecanoate) in water

Rati Ranjan Nayak · Sumita Roy · Joykrishna Dey

Received: 18 February 2006 / Accepted: 31 May 2006 / Published online: 2 September 2006  
© Springer-Verlag 2006

**Abstract** A polysoap poly(sodium 11-acrylamidoundecanoate) was synthesized from sodium 11-acrylamidoundecanoate in water. The molecular weight of the polymer was determined by gel permeation chromatography and static light scattering techniques. Fluorescence probe studies in water have suggested the formation of hydrophobic domains within the same polymer chain. The microenvironment of the hydrophobic domains is highly ordered. The packing of the hydrocarbon chains in the hydrophobic domains formed by intra-chain association increases upon decrease of pH. The transmission electron micrograph revealed large vesicular aggregates in dilute aqueous solution. Temperature-dependent fluorescence anisotropy of the 1,6-diphenyl-1,3,5-hexatriene probe demonstrated stability of the vesicles.

**Keywords** Polysoaps · Fluorescence · Vesicles

## Introduction

In aqueous solution, above a critical concentration, amphiphilic molecules self-assemble to form a variety of microstructures such as micelles, vesicles, tubules, and rods etc. The microstructures formed by the amphiphiles are in dynamic equilibrium with the surfactant monomer in solution. One way to obtain structural stabilization of molecular self-assemblies is chemically tethering the surfactant monomers through polymerization. To be able to do so, surfactant monomers that incorporate a polymerizable group such as vinyl moiety are required. The short

chain surfactant monomers can then be incorporated into the polymer backbone through polymerization of the vinyl group. Interests in micellar polymerization arise from the expectation that stable micelles may be produced for some technological applications. Synthesis of various cationic and anionic polymerized micelles has been reported in the literature. Polymeric soaps with a number average molecular weight of about 2000 Da are referred to as ‘polymeric micelles’ and those with high molecular weight ( $10^5$ – $10^6$  Da) are called ‘polysoaps’ [1]. Polymeric soaps are capable of forming both intra-chain and inter-chain aggregates of a variety of morphologies. Several studies on polymerizable anionic and cationic surfactants have been recently reviewed [2]. Some strong surface-active polymerizable monomers (e.g. 10-*p*-styryl undecanoate, 9-acrylamido stearate, sodium sulfodecylstyrlyl ether and styryloxydecyltrimethylammonium bromide) have been reported [3]. Polymerization of surfactants such as sodium acrylamido stearate [4] sodium acrylamidoundecanoate [5], quaternary alkyl salts of dimethylaminomethyl methacrylate with different alkyl chain length [6, 7] have also been reported. Most of these surfactants were polymerized in normal micelles [5, 7]. However, surface tension studies of these polymers suggested that they do not form micelles. That is, the poly(sodium acrylamidoalkanoate)s, in fact, act as anionic polyelectrolytes in water. The performances of these anionic polyelectrolytes as coagulant aids in conjunction with alum in water treatment have been assessed. All these polyelectrolytes tested in water treatment [8] are as effective as that of commercially available cationic polyamine organic coagulants. Poly(sodium acrylamidoalkanoate)s have also utilities as water-soluble viscosifiers and displacement fluids in enhanced oil recovery.

Recently, we have shown that the vesicle structure formed by sodium *N*-(11-acrylamidoundecanoyl)-L-alani-

R. Nayak · S. Roy · J. Dey (✉)  
Department of Chemistry, Indian Institute of Technology,  
Kharagpur 721 302, India  
e-mail: joydey@chem.iitkgp.ernet.in

nate in water [9] is retained even after polymerization to form poly[sodium *N*-(11-acrylamidoundecanoyl)-L-alaninate] [10]. Our studies have also shown that sodium acrylamidoundecanoate (SAU) forms bilayer vesicles in aqueous solution [11]. For the present study, the corresponding polysoap, poly(sodium acrylamidoundecanoate), PSAU (see Fig. 2 for chemical structure), was chosen in order to understand the aggregation behavior of poly(sodium acrylamidoalkanoate)s in water. The major objective of this study is to examine if the polysoap in aqueous solution retains the vesicular structure of the monomeric surfactant.

## Experimental section

### Materials

Acryloyl chloride, and 11-aminoundecanoic acid were used as obtained from Aldrich. Uranyl acetate was obtained from MERK, Germany. The fluorescence probes pyrene, 1,6-diphenyl-1,3,5-hexatriene (DPH), and *N*-phenyl-1-naphthylamine (NPN) were purchased from Aldrich and were used after recrystallization at least three times from ethanol or acetone–ethanol mixture. Purity of all the probes was tested by the fluorescence emission and excitation spectra. Analytical grade sodium hydroxide, sodium bicarbonate, sodium dihydrogen phosphate, disodium hydrogen phosphate, sodium acetate, sodium chloride, hydrochloric acid were procured from SRL and were used directly from the bottle. Milli-Q water (18.2 MΩ) obtained from Millipore water purification system was used for all the experiments.

### Synthesis of polysoaps

The synthesis and purification of SAU has been reported in our earlier paper [11]. PSAU was obtained by free-radical polymerization of SAU well above its critical vesicle concentration (3.45 mM) [11] in water using K<sub>2</sub>S<sub>2</sub>O<sub>8</sub> as radical initiator under N<sub>2</sub> atmosphere at 60 °C according to the procedure reported elsewhere [5]. The polymer solution was dialyzed for 72 h using 12 kDa molecular weight cut off dialysis bag against alkaline water (pH=10) with frequent change of water and then lyophilized to get dry PSAU. The polymerization was confirmed by the disappearance of the vinyl proton peaks between δ values 5.0 and 7.0 in the <sup>1</sup>H NMR spectrum of PSAU in D<sub>2</sub>O. Also the broadness of the peaks suggested a polymeric structure of PSAU. Further, the FT-IR spectrum of the polymer showed no C=C stretching frequency around 1620 cm<sup>-1</sup> confirming the polymeric structure.

### Measurements

#### Gel permeation chromatography

For molecular weight determination by GPC the protonated form of the polysoap, PSAU was employed. GPC was performed at 40 °C with a setup consisting of a waters 515 HPLC pump and High MW column: Polymer Labs-Plgel 5 μm Mixed C (300×7.5 mm). The isocratic flow rate was set at 1.0 mL/min using uninhibited DMF as the mobile phase and the elution of the sample was monitored with RI (refractive index) detector. The elution times were converted to molecular weights with a calibration curve constructed from narrow polydispersity polymethylmethacrylate (PMMA) standards (High MW standards: Polymer Labs-(M-M-10 Kit: 1000–1.5 m range). A dilute polymer solution (0.033%) prepared in DMF was injected into the 20 μL sample loop. The calculation of molecular weight and polydispersity index was done by Waters Millennium software (version 4.0).

#### Static light scattering measurements

Static light scattering (SLS) measurements were performed with a Photol DLS-7000 (Otsuka Electronics Co. Ltd., Osaka, Japan) optical system equipped with an Ar<sup>+</sup> ion laser (75 mW) operated at 16 mW at λ=488 nm, a digital correlator, and a computer-controlled and stepping-motor-driven variable angle detection system. The instrument was calibrated with toluene for which the Rayleigh ratio is well-known ( $40 \times 10^{-6} \text{ cm}^{-1}$  at 488 nm) [12]. For SLS measurements, a stock solution of the polysoap was prepared in Milli-Q water. Then it was diluted to the desired concentrations. The solutions were filtered through a micro-syringe filter (0.22 μm) to the scattering cell. The refractive index increments of the sample solutions were determined by use of a double beam differential refractometer (DRM-1021, Photol, Otsuka Electronics). Measurements were made at 10 different angles from 45 ° to 135 ° for each of the polymer solutions.

In the static light scattering experiment, laser light is scattered by macromolecules or particles such as colloids in solution. The intensity of the scattered light is a function of the nature of the molecules, their size, molecular weight, shape, concentration, and possible additional parameters. When the molecule become larger, approximately 1/20 the wavelength of the incident light, the scattered intensity becomes also a function of the scattering angle, the angle between the incident and scattered light, due to intermolecular interference. The reciprocal of the scattered intensity can be expressed by the Zimm equation [13]:

$$KC/R_\theta = 1/M_w(1 + 1/3 < R_g^2 >_z q^2) + 2A_2C \quad (1)$$

where  $K$  is an optical constant, expressed as  $K=2\pi^2n^2(dn/dC)^2/(N_A\lambda^4)$ , and  $q=(4n/\lambda) \sin(\theta/2)$  with  $N_A$ ,  $dn/dC$ ,  $n$ , and

$\lambda$  being Avogadro's number, the specific refractive index increment, the solvent refractive index, and the wavelength of light in vacuum, respectively.  $R_\theta$  known as the excess Rayleigh ratio, is the angular dependence of the excess absolute time-averaged scattered intensity.  $C$  is the polymer concentration (grams per milliliter).  $\langle R_g^2 \rangle_z^{1/2}$  is the root-mean-square  $z$ -average radius of gyration. A corresponding Zimm plot yields for the appropriate extrapolation the weight average of the molecular weight  $M_w$ . On the basis of the SLS theory, for a relatively dilute polymer solution or strongly interacting particles (for example, polyelectrolytes) Eq. (1) can be expressed as

$$KC/R_\theta = 1/M_w + 1/(3M_w) \langle R_g^2 \rangle_z q^2 \quad (2)$$

In the present study, because of very dilute polymer solutions, the apparent radius of gyration was calculated after measuring  $R_\theta$  at a set of  $\theta$  using Eq. (2). The weight average molecular weight was obtained as the inverse of the intercept of the plot (not shown) of reciprocal scattering intensity ( $KC/R_\theta$ ) vs  $\sin^2\theta/2$  for  $0.025 \text{ g L}^{-1}$  polymer solution.

#### Steady-state fluorescence spectra

The steady-state fluorescence spectra were recorded in a SPEX Fluorolog-3 spectrophotometer. The solutions containing pyrene were excited at 335 nm and emission intensity was measured in the wavelength range of 350 nm to 500 nm. On the other hand, the fluorescence spectra of NPN were obtained by excitation at 350 nm. Each spectrum was blank subtracted and was corrected for lamp intensity variation during measurement. The excitation and emission slit widths were both set at 1 nm for pyrene and 2.5 nm for NPN. The fluorescence anisotropy measurements were performed with a Perkin Elmer LS-55 spectrophotometer equipped with a thermostating, magnetically stirred cell housing that allowed temperature control of  $\pm 0.1^\circ\text{C}$  using a Thermo Neslab RTE-7 circulating water bath. The sample was excited at 350 nm and the emission intensity was followed at 450 nm using excitation and emission slits with band-pass of 2.5 nm and 2.5–5.0 nm, respectively. The steady-state fluorescence anisotropy values ( $r$ ) were calculated employing the equation:

$$r = (I_{VV} - GI_{VH})/(I_{VV} + 2GI_{VH}) \quad (3)$$

where,  $I_{VV}$  and  $I_{VH}$  are the fluorescence intensities polarized parallel and perpendicular to the excitation light, and  $G$  ( $= I_{VV}/I_{VH}$ ) is the instrumental grating factor. The software supplied by the manufacturer automatically determined the correction factor and anisotropy value. In all cases, the anisotropy values were averaged over an integration time of 10 s and a maximum number of six measurements for each sample. A 2 mM solution of the

probe was prepared in 20% methanol–water mixture. The final concentration of the probe was adjusted to  $2 \mu\text{M}$  by addition of an appropriate amount of the stock solution. The anisotropy measurements were carried out at different polymer concentrations in the temperature range  $20$ – $60^\circ\text{C}$ . Before measurement started the solution was equilibrated 10 min at a particular temperature.

#### Transmission electron microscopy (TEM)

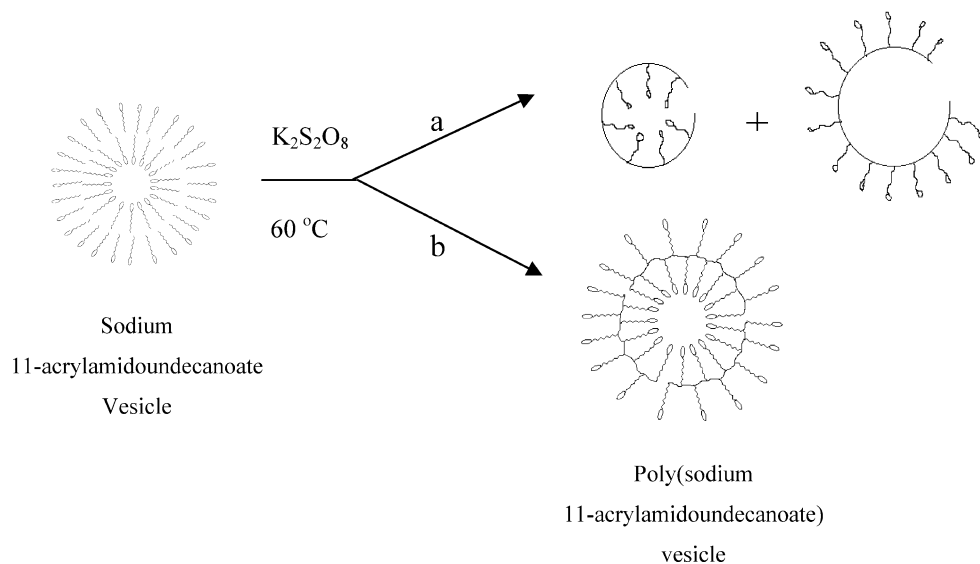
The electron micrographs of the specimens were examined on an electron microscope (Phillips CM 200) operating at an accelerating voltage of 200 kV at room temperature ( $\sim 25^\circ\text{C}$ ). The specimen for TEM measurements was prepared after equilibration of the polymer solution for 2–3 h. A carbon-coated copper grid was immersed in a drop of aqueous solution of the polymer for 1 min, blotted with filter paper, air-dried, and negatively stained with freshly prepared 1.0% aqueous uranyl acetate. The specimens were air-dried for an hour and then examined under the microscope.

## Results and discussion

#### Molecular weight of PSAU

Since the surfactant monomer forms bilayer vesicles in water [11], polymerization can either take place among surfactant monomers in the same layer (i.e. linear polymerization) or by zipping-up of the monomers of both layers of the bilayer assembly (see Fig. 1). In the latter case, the molecular weight is expected to be higher. The molecular weight of the polysoap was obtained by gel permeation chromatography (GPC). The weight average and number average molecular weights thus obtained are  $6.30 \times 10^6$  and  $5.85 \times 10^6$ , respectively. The polydispersity index (PDI) is about 1.08. Low PDI value suggests narrow molecular weight distribution. This is because polymerization occurred in the aggregate form of the monomers. Also dialysis of the sample ensured low PDI value. The molecular weight was also determined by SLS method using polymer solutions in the concentration range of  $0.025$ – $0.1 \text{ g L}^{-1}$ . The Zimm analysis resulted in a weight average molecular weight of  $1.57 \times 10^7$  with an error of 32%. This might be due to inter-chain aggregation at higher concentrations of the polymer. Therefore, we constructed the Berry plot (not shown) using the scattering data of the dilute ( $0.025 \text{ g L}^{-1}$ ) aqueous solution of PSAU to ensure absence of any aggregates. This gave a weight average molecular weight of  $6.93 \times 10^6$ . The molecular weight values obtained by GPC and SLS methods are very close to each other. Similar values are also reported in the

**Fig. 1** Mechanism of polymerization of SAU by (a) linear and (b) zipping-up process



literature [13, 14]. The high molecular weight of the polysoap may be taken as an evidence of zipping-up rather than linear polymerization of bilayer vesicles.

#### Hydrophobic domain formation

In aqueous solution, the surfactant units in the polymer chain can assemble in a way to form unimolecular micelles. This process is expected to be concentration-independent. On the other hand, the polymer chains can also undergo concentration-dependent self-organization to form inter-chain aggregates. In order to examine the formation of hydrophobic domains, fluorescence probe studies were performed using NPN as a probe molecule. Though NPN is weakly fluorescent in aqueous solution, its fluorescence spectrum in the presence of PSAU shows a huge increase in

intensity accompanied by a large spectral shift toward shorter wavelengths relative to that in water. This suggests that the probe molecules are solubilized in nonpolar environments [15, 16]. The shift ( $\Delta\lambda = \lambda_{water} - \lambda_{sol}$ ) of the emission maximum is plotted as a function of polymer concentration in Fig. 2. Absence of any concentration-independent region at low polymer concentrations suggests formation of hydrophobic domains within the same polymer chain. This is possible only if self-association of the pendent amphiphilic groups of the polymer chain takes place. The plot shows that the onset of inter-chain aggregation occurs at a polymer concentration of  $\sim 0.05\text{ g L}^{-1}$ , which can be taken as the critical aggregation concentration (CAC) of the polysoap.

#### Transmission electron microscopy

The TEM picture (Fig. 3) of the dilute aqueous solution containing  $0.02\text{ g L}^{-1}$  PSAU reveals closed spherical vesicles

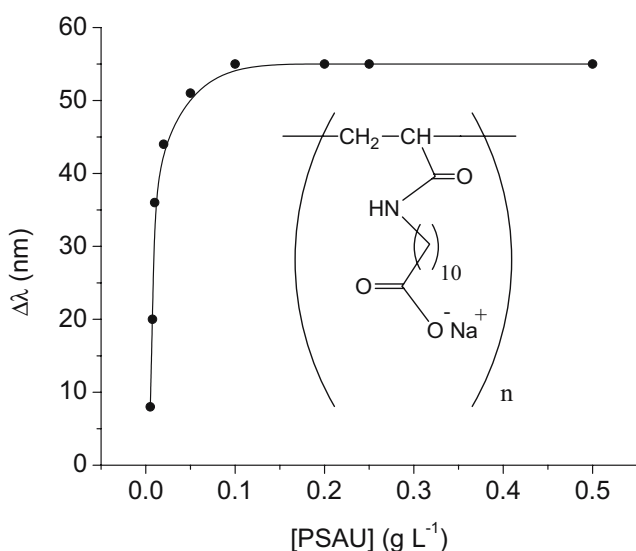


**Fig. 2** Plot of shift of fluorescence emission maximum ( $\Delta\lambda$ ) of NPN against polymer concentration; inset: chemical structure of PSAU

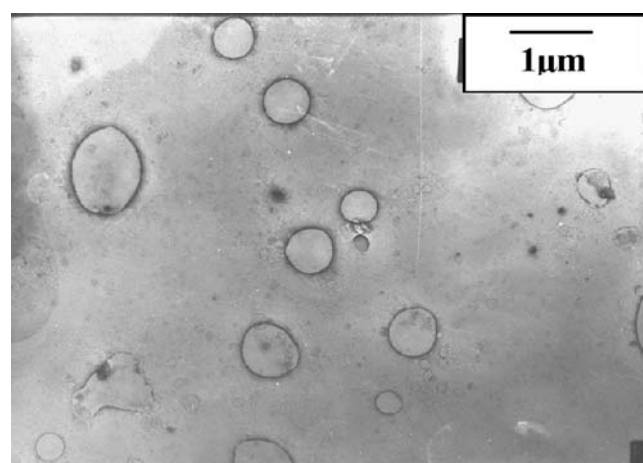


**Fig. 3** Negatively stained (with 1% uranyl acetate) TEM micrograph of  $0.02\text{ g L}^{-1}$  aqueous solution ( $\text{pH}=6.0$ ) of PSAU

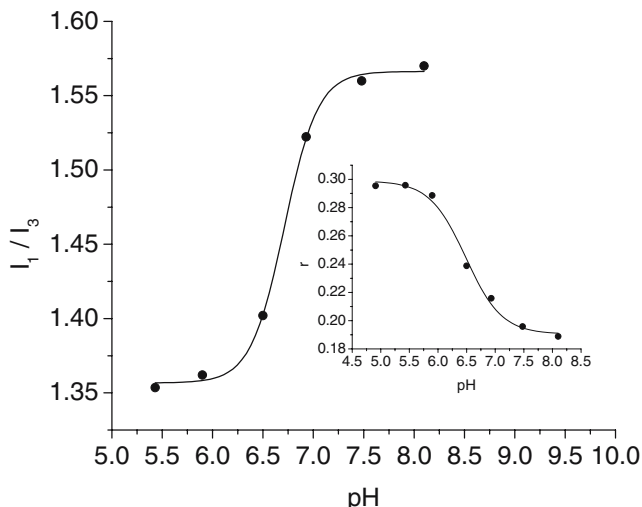


**Fig. 4** pH dependence of polarity ratio ( $I_1/I_3$ ) in  $0.02 \text{ g L}^{-1}$  PSAU; inset: pH dependence of anisotropy ( $r$ ) in  $0.02 \text{ g L}^{-1}$  PSAU

of different sizes (inner diameter=300 nm–1.2  $\mu\text{m}$ ). However, no identifiable structure was observed in the micrograph (not shown) of the concentrated ( $0.25 \text{ g L}^{-1}$ ) solution of PSAU.

#### pH and temperature dependence of aggregation

Since the polysoap has carboxylate groups, there might be an influence of pH on microstructure formation. The micropolarity of the hydrophobic domains depends upon the microstructure of the self-assemblies. It has been reported that the change of  $I_1/I_3$  ratio of pyrene fluorescence can be used to study hydrophobic domain formation [17, 18]. Therefore, the polarity ratio  $I_1/I_3$  was measured in the presence of the polysoap at different pH. In dilute solution ( $0.02 \text{ g L}^{-1}$ ) of the polysoap, the ratio (1.57), which is much lower than in pure water (1.81) decreased at pH < 8 (Fig. 4). This means that the probe molecule is solubilized in a less polar environment and the microenvironment around the probe molecule becomes more hydrophobic at low pH. Similar observation was also made with the monomeric surfactants and can be attributed to the change in the ionization state of the carboxylate group. The decrease of ionization at lower pH results in a decrease of charge repulsion and hence tighter packing of the hydrocarbon chains thereby preventing water penetration. That is, the intra-chain aggregate has a more compact structure at lower pH. The pH corresponding to the inflection point can therefore be taken as the  $pK_a$  (6.7) of the carboxylic acid group. The  $pK_a$  value thus obtained is very close to the corresponding value of the monomeric surfactant [11], which means that the pendent surfactant units are not free. They are part of aggregate structures that have high negative charge density. This implies formation of closed bilayer structures in aqueous solution.

This has been further demonstrated by fluorescence anisotropy studies described below.

The enhanced chain packing in the hydrophobic domains formed by the polysoaps is also manifested by the fluorescence anisotropy of the DPH probe. The steady-state fluorescence anisotropy ( $r$ ) of DPH was measured in polymer solution ( $0.02 \text{ g L}^{-1}$ ) at different pH. The variation of  $r$  with pH is shown as an inset of Fig. 4. It is important to note that the fluorescence anisotropy of the DPH probe increases with the decrease of pH of the polymer solution. This is consistent with the decrease in micropolarity of the hydrophobic domains as discussed in the preceding paragraph. The protonation of the carboxylate groups reduces the charge at the surface that strengthens the amide hydrogen-bonding interaction between two surfactant units making the packing of the hydrocarbon chains tighter. The  $pK_a$  (6.5) value obtained from the inflection point of the plot, within the experimental error limit, is equal to the value obtained from the fluorescence titration of pyrene. The  $r$  value was found to be closely equal to those of liposomes [19]. The relatively high value of  $r$  in dilute polymer solution suggests an ordered environment around the DPH probe in the assemblies. That is the hydrocarbon chains of the surfactant units are tightly packed in the intra-chain aggregates. It should also be noted here that the  $r$  value in the presence of polysoap is higher compared to that found for the monomeric counterpart [11]. This suggests that the bilayer structures are retained after polymerization of the surfactant monomers. Others have also reported a decrease of membrane fluidity in polymerized vesicles [20]. Low fluidity of the membrane also provides evidence of zipping-up rather than linear polymerization of bilayer vesicles.

The plot in Fig. 5 shows that there is a very little decrease of  $r$  value with the rise of temperature. It is interesting to

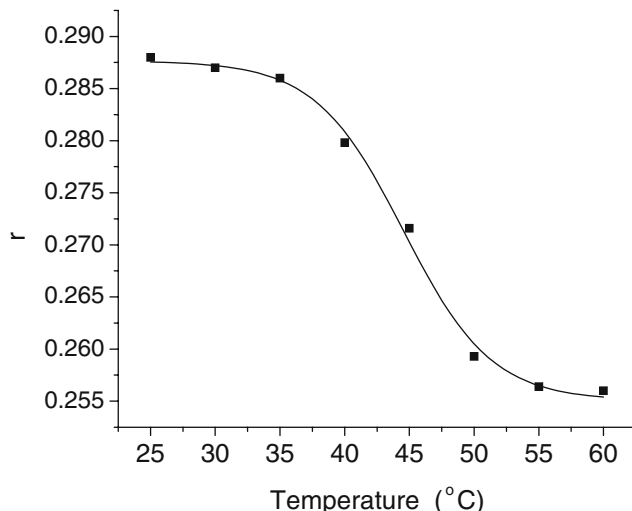


**Fig. 5** Plot of anisotropy ( $r$ ) of DPH vs temperature in aqueous solution (pH 6.0) of PSAU ( $0.02 \text{ g L}^{-1}$ )

note that even at high temperature, the anisotropy value is above 0.25, which suggests that the bilayer structure of the vesicles is retained. That is, the vesicles are very stable. The small change of  $r$  is due to hydrocarbon chain mobility. Thus the temperature corresponding to the inflection point of the sigmoid curve can be taken as the transition temperature,  $T_m$  (45 °C) between the two states.

## Conclusion

We have synthesized a polysoap from the surfactant monomer SAU that forms bilayer vesicles in water. High molecular weight of the polysoap suggests that the polymerization occurs by zipping-up of the monomers in both layers of the bilayer vesicles. The bilayer structure is retained after polymerization. As in the case of SAU the vesicle formation of the polysoap is favored below neutral pH. The  $pK_a$  of the carboxylic groups was found to be almost two orders of magnitude higher than that of corresponding free alkanoic acid. The vesicles formed by the polysoap are very stable against the rise of temperature. Therefore, the polysoap may have potential uses as drug delivery vehicle.

**Acknowledgements** The work reported in this paper was supported by the CSIR (Grant No. 01(1664)/00/EMR-II). S.R thanks the CSIR for a research fellowship (9/81(380)/2002-EMR-I). RRN is thankful to the IIT, Kharagpur for a research associateship.

## References

1. Larrabee CE, Sprague ED (1979) *J Polym Sci Polym Lett Ed* 17:749
2. Paleos CM, Malliaris A (1988) *J Macromol Sci Rev Macromol Chem Phys C* 28:403
3. Tasaur SL (1983) Ph. D. Thesis, University Microfilms International
4. Chew CH, Gan LM (1985) *J Polym Sci Polym Chem Ed* 23:2225
5. Yeoh KW, Chew CH, Gan LM, Koh LL, Teo HH (1989) *J Macromol Sci Chem A* 26:663
6. Nagai K, Ohishi Y, Inaba H, Kudo S (1985) *J Polym Sci Polym Chem Ed* 23:1221
7. Nagai K, Ohishi Y (1987) *J Polym Sci Part A Polym Chem* 25:1
8. Gan LM, Yeoh KW, Chew CH, Koh LL, Tan TL (1991) *J Appl Polym Sci* 42:225
9. Roy S, Dey J (2005) *Langmuir* 21:10362
10. Nayak RR, Roy S, Dey J (2005) *Polymer* 46:12401
11. Roy S, Dey J (2003) *Langmuir* 19:9625
12. Cummins HZ, Pike ER (Eds) (1974) *Photon correlation and light beating spectroscopy*. Plenum, New York
13. Zimm BH (1948) *J Chem Phys* 16:1099
14. Fujimoto C, Fujise Y, Kawaguchi S (2000) *J Chromatogr A* 871:415
15. Gan LM, Chew CH (1992) Organized solutions. In: Friberg SE, Lindman B (eds) *Surfactant science series*, vol 44. Marcel Dekker, Inc., New York, pp 327
16. Tohru S, Keita T, Masataka H (2002) *Anal Chim Acta* 454:203
17. Huang J, Bright FV (1992) *Appl Spectrosc* 46:329
18. Dong DC, Winnik MA (1982) *Photochem Photobiol* 35:17
19. Winnik FM, Regismond STA (1996) *Colloid Surf A* 118:1
20. Shinitzky M, Barenholz Y (1974) *J Biol Chem* 249:2652
21. Kusumi A, Singh M, Tirrell DA, Oehme G, Singh A, Samuel NKP, Hyde JS, Regen SL (1983) *J Am Chem Soc* 105:2975